The effect of crystallographic orientation on solid metal induced embrittlement of Ti-6Al-1Mo-1V in contact with copper

The effect of crystallographic orientation on solid metal induced embrittlement of Ti-8Al-1Mo-1V in contact with copper

To cite this article: P Åkerfeldt *et al* 2013 *IOP Conf. Ser.: Mater. Sci. Eng.* **48** 012011

IOP Conf. Series: Materials Science and Engineering **48** (2013) 012011 doi:10.1088/1757-899X/48/1/012011

The effect of crystallographic orientation on solid metal induced embrittlement of Ti-8Al-1Mo-1V in contact with copper

P Åkerfeldt[1]*, R Pederson[1,2] , M-L Antti[1], Y Yao[3] and U Klement[3]
[1]Division of Materials Science, Luleå University of Technology, SE 97181 Luleå, Sweden
[2]Research & Technology Centre, GKN Aerospace Engine Systems, SE 46181 Trollhättan, Sweden
[3]Department of Materials and Manufacturing Technology, Chalmers University of Technology, SE 41296 Göteborg, Sweden

*Corresponding author: pia.akerfeldt@ltu.se

Abstract. Solid metal induced embrittlement (SMIE) occurs when a metal experiences tensile stress and is in contact with another metal with lower melting temperature. SMIE is believed to be a combined action of surface self-diffusion of the embrittling species to the crack tip and adsorption of the embrittling species at the crack tip, which weakens the crack tip region. In the present study, both SMIE of the near alpha alloy Ti-8Al-1Mo-1V in contact with copper and its influence by crystallographic orientation have been studied. U-bend specimens coated with copper were heat treated at 480°C for 8 hours. One of the cracks was examined in detail using electron backscatter diffraction technique. A preferable crack path was found along high angle grain boundaries with grains oriented close to [0001] in the crack direction; this indicates that there is a connection between the SMIE crack characteristics and the crystallographic orientation.

1. Introduction

Metal induced embrittlement (MIE) can occur when a metal experiences tensile stress and is in contact with a metal of lower melting temperature. What distinguishes MIE is that normally ductile metals become brittle in contact with metals under certain conditions [1] and that the degradation is often undetected until the catastrophic failure occurs [2]. There are two types of MIE: embrittlement that occurs above the melting temperature of the embrittling metal (T_m), referred to as liquid metal embrittlement, and embrittlement that occurs below T_m, known as solid metal induced embrittlement (SMIE) [1,3,4]. SMIE has been investigated in the present study.

The essential condition for SMIE to occur is intimate contact between the embrittling metal and the metal substrate [2,4-8]. In order to promote SMIE, any oxides present must first be removed either chemically or mechanically. The service temperature (T) and the amount of tensile stress present are also influencing parameters; below certain threshold values, SMIE is not expected to take place [1,5,9,10]. The crack propagation rate of SMIE increases with increasing temperature, and is highest just below T_m [4,6,9]. However, the severity of SMIE is also dependent on the distance between the source of the embrittling species and the crack tip. If embrittling species are present as inclusions the crack propagation rate has been found to be high [4,7], whilst severity is expected to decrease with

increasing crack length when embrittling species are present as thin films on the surface [7]. The mechanism of SMIE is believed to be a combination of surface self-diffusion of the embrittling species to the crack tip [3,7,11,12] and adsorption of the embrittling species at crack tip [4,5,7,11]. It is generally agreed that adsorption of the embrittling metal leads to a weakening of the crack tip, but exactly how adsorption affects the crack propagation is not fully understood. Two principal theories are: (1) chemisorption reduces the stress required for tensile separation of the atoms at the crack tip leading to decohesion [1,13-15], and (2) chemisorption facilitates the nucleation or egress of dislocations at the crack tip [11,16-19].

SMIE of titanium alloys in contact with the following solid materials has been observed: silver, gold, copper and cadmium, see table 1. In 1965 Duttweiler et al. [20] concluded that the failure of titanium compressor discs resulted from SMIE caused by silver chloride. Additional studies showed that Ti-5Al-2.5Sn, Ti-8Al-1Mo-1V and Ti-7Al-4Mo alloys all exhibited SMIE when in contact with solid silver. Embrittlement caused by solid silver has also been studied by Stoltz and Stulen [21], who observed SMIE of Ti-6Al-6V-2Sn in contact with solid silver, gold and cadmium. Meyn [22], and Fager and Spurr [10] have reported SMIE caused by cadmium in contact with Ti-8Al-1Mo-1V, Ti-6Al-4V and Ti-3Al-14V-11Cr. Most recently however, the influence of solid copper has been studied; Liu [23] reported in 2006 that solid copper caused SMIE of Ti-6.5Al-3.5Mo-1.5Zr-0.3Si. The present work is a continuation of a previous study of SMIE in Ti-6Al-2Sn-4Zr-2Mo and Ti-8Al-1Mo-1V in contact with copper and gold [24]. Although SMIE has been observed in previous studies, crack propagation behaviour in relation to crystallographic orientation has not been evaluated; this is the aim of the present study.

Table 1. Previous investigations of titanium alloys and embrittling species.

Alloy	Solid embrittling species
Ti-5Al-2.5Sn	Ag [20]
Ti-8Al-1Mo-1V	Ag [20], Au [24] Cd [22], Cu [24]
Ti-6Al-4V	Cd [22]
Ti-6Al-6V-2Sn	Ag [21], Au [21], Cd [21]
Ti-6Al-2Sn-4Zr-2Mo	Au [24], Cu [24]
Ti-6.5Al-3.5Mo-1.5Zr-0.3Si	Cu [23]
Ti-7Al-4Mo	Ag [20]
Ti-3Al-14V-11Cr	Cd [22]

2. Materials and Method

A U-bend test was used to evaluate SMIE of Ti-8Al-1Mo-1V in contact with copper. The sheet material, condition and composition were in accordance with AMS4916J [25] and were statically loaded by U-bending, and then coated with 0.05-0.1 μm solid copper using sputtering technique. Specimens were subsequently heat treated at 480°C for 8 hours; details of the test method can be found in previous work [24]. Principal metallographic examination was performed in a light optical microscope at 500x magnification. The outer surface of the cross-section of the U-bend shape was examined for cracking and the locations of the observed cracks noted.

Specimens exhibiting cracking were further examined in a scanning electron microscope (SEM, LEO 1550 Gemini FEG-SEM). The cracks were studied by using backscattered electron imaging (BSE) with high contrast, which allowed the alpha and beta phases to be discriminated by compositional contrast without etching. Electron backscatter diffraction (EBSD), a characterisation technique employed in the SEM, was used to determine the local crystallographic orientation and the texture of the area of interest along the crack propagation path in a specimen. For EBSD mapping an HKL Channel-5 EBSD system with a Nordlys II detector was used. Two orientation maps were

acquired at 5000x magnification with an accelerating voltage of 20 kV and a step size of 200 nm. An average noise reduction of four neighbours was applied.

3. Results

In figure 1 a), the BSE image of a typical crack path is shown. Alpha and beta phase can clearly be discriminated by the compositional contrast as grey and white, respectively. For a better understanding of the crack propagation characteristics, EBSD measurements were performed along the crack path. To the right in figure 1, band contrast images are shown obtained at area A and B, which clearly shows that the crack is mainly propagating along the grain boundaries.

Two orientation maps were acquired along the crack path and in the respective inverse pole figures in Y-direction, the orientations of the grains along the crack were found to be close to [0001]. In figure 2 a), the orientation maps given in inverse pole figure scheme are stitched together to create a map including the whole crack path. According to the inverse pole figure colour scheme given in figure 3, the grains with the orientation close to [0001] are coloured red. In the phase map (figure 2 b)), the

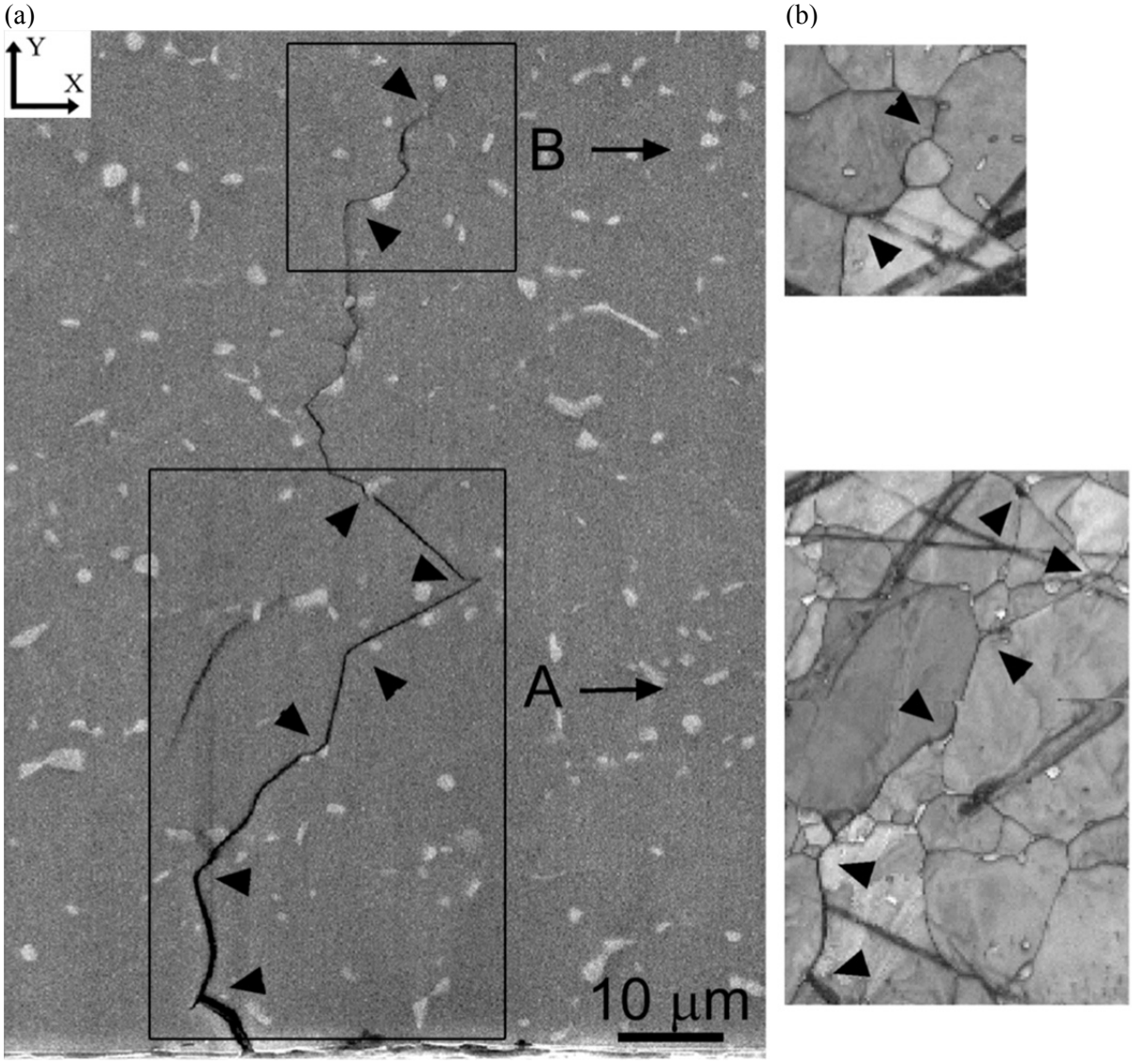

Figure 1. (a) The typical appearance of the SMIE of Ti-8Al-1Mo-1V in contact with copper and (b) the band contrast images of area A and B indicating how the crack is propagating along the grain boundaries.

alpha and the beta phases are coloured blue and red, respectively, and the orientations of the grains along the crack path represented by the unit cell. The grain boundaries in the orientation map in figure 2 a) are defined by the degree of misorientation (θ) between two neighbouring pixels. The high-angle grain boundaries (θ>10°) are given as black lines while the low-angle boundaries (3°<θ<10°) by white lines. The EBSD results indicate that the crack path is following high-angle grain boundaries and there is a tendency of the crack to propagate along [0001]-oriented grains (along Y-direction).

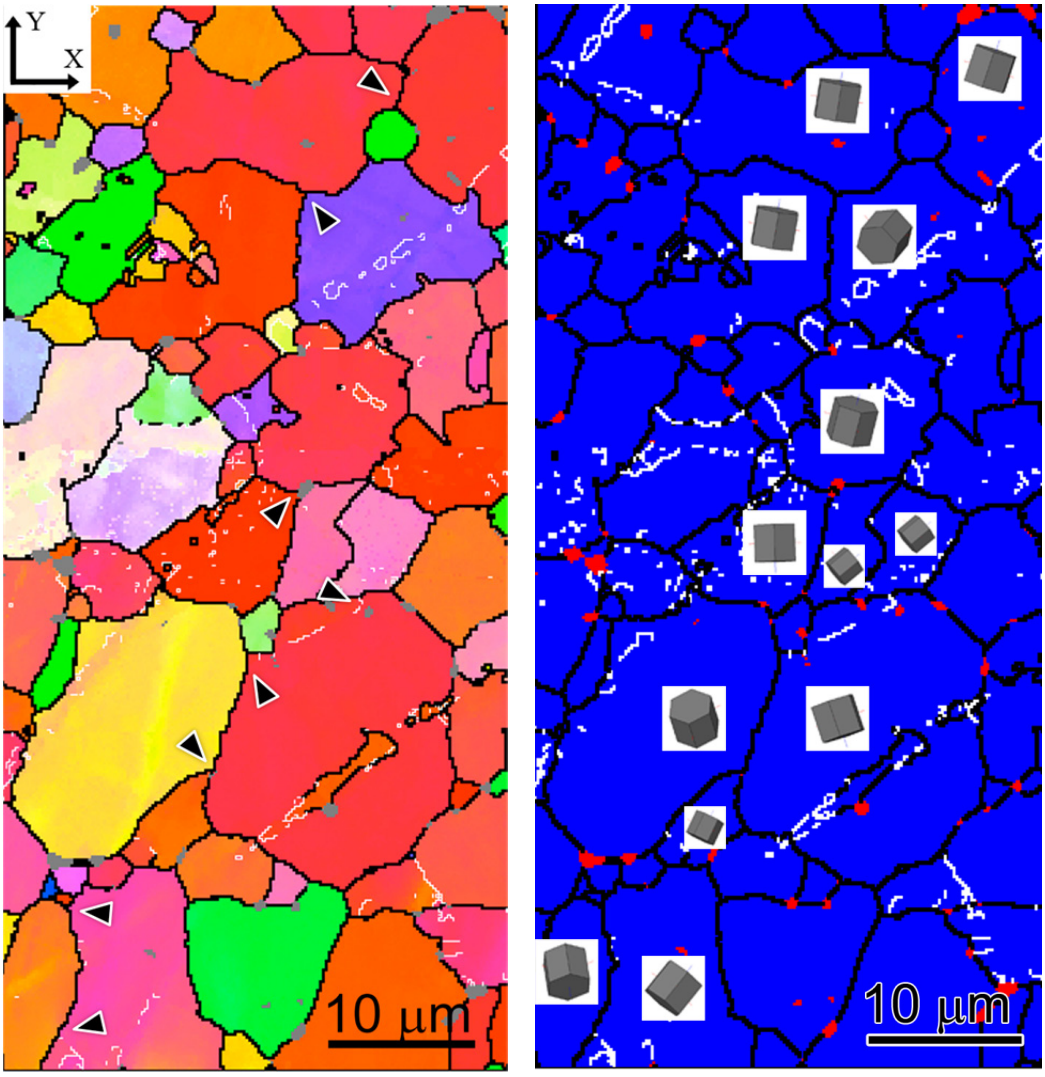

(a) **(b)**

Figure 2. (a) Orientation map in inverse pole figure colour code and (b) phase map with grain orientations along the crack path represented by their respective unit cells.

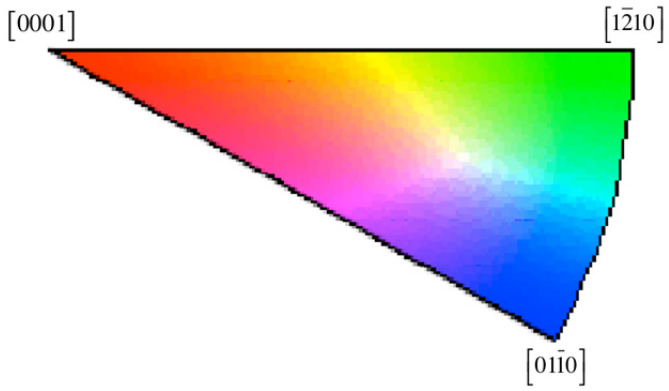

Figure 3. Inverse pole figure colour scheme used for the orientation map in figure 2.

4. Discussion

Metals with hcp (hexagonal close-packed) crystallographic structure such as alpha titanium (see grey phase in figure 1), normally fracture by cleavage fracture [26]. In this study the crack growth path was found to be intergranular, which itself is a clear indication that there is an influence of an embrittling environment. The crack propagates along grain boundaries, perpendicular to the surface and loading direction, i.e. in a direction towards high stress levels. The embrittling environment in the present study was solid copper. During heat treatment in air at 480°C however, the copper layer oxidises and consequently the embrittling species closest to the titanium surface are in the form of CuO, Cu_2O, and Cu, see figure 4. Because of the strong reducing properties of titanium, the copper oxide closest to the titanium surface is probably reduced to form titanium oxide and copper:

$$2Cu_2O(s) + Ti(s) \rightleftharpoons 4Cu(s) + TiO_2(s) \quad (1)$$

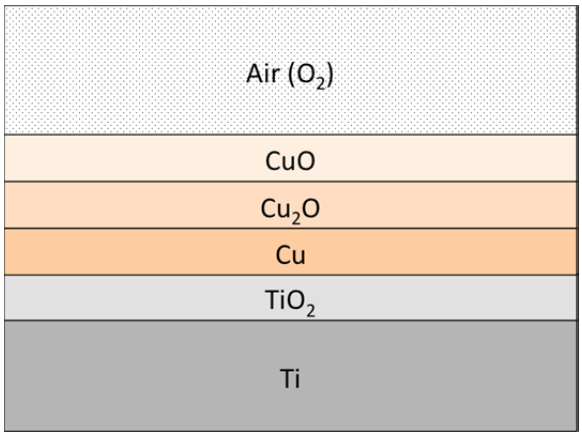

Figure 4. The assumed surface composition after heat treatment in air.

Once the crack is initiated, the embrittling species are believed to be transported by surface self-diffusion to the crack tip and adsorption of the embrittling species at the crack tip weakens the crack

tip region. In previous work the characteristic self-diffusion length of copper for 8 hours at 480°C, has been calculated to be 2300 μm [27]. Hence, the diffusion length is longer than the crack length observed in the experimental study. When comparing the characteristic diffusion length with the experimental crack length however, one should also consider the incubation time and the fact that the experimental crack is following a serrated path making the crack much longer than what it first appears as. In addition the amount of copper available for surface self-diffusion needs to be taken into account since the presence of copper at the crack tip is crucial for crack growth to occur. The relationship between crack length and amount of copper available can be estimated using the following simple stoichiometric calculation. Assume that the crack is two-dimensional and that the copper atoms originate from a layer of copper atoms 10 μm wide (w) and 0.05 μm thick (t) at the surface. Moreover, assume that the crack wall is covered with at least five atom layers of copper, this to sustain the SMIE crack propagation rate. Thus, at least ten atom layers (N) are required for self-diffusion of copper along our two-dimensional crack. The estimated crack length, L_{crack}, can then be calculated:

$$L_{crack} = \frac{wt}{Nd} = \frac{10 \cdot 0{,}05}{10 \cdot 0{,}000256} \approx 200\mu m \quad (2)$$

where the diameter of a copper atom (d) being 0.000256 μm. Thus, with an estimated thickness of sputtered copper layer of 0.05 – 0.1 μm, the calculated stoichiometric crack length lies between 200 and 400 μm. Taking the diffusion rate and availability of copper atoms into consideration, the transport mechanism of surface self-diffusion appears to be applicable for the present results.

The mechanism of adsorption at the crack tip is complex. It is generally agreed that chemisorption of the embrittling species weakens the crack tip region, but exactly how is debatable [1,17]. The result of this EBSD study shows that the crack propagates principally along high-angle grain boundaries, which is in agreement with theories of adsorption: the thermodynamic driving force for adsorption is the reduction in surface free energy, which is larger for high-angle grain boundaries [28]. However, when the orientation of grains along the crack path is considered, a favourable crack growth is observed along grains oriented close to [0001] in Y-direction (see figure 2). A possible reason may be the coordination number of the bulk atoms, which influences surface energy. Along the crack there is a layer of copper and copper oxides, see figure 5, and at the interface of the crack tip both oxygen and copper atoms bond to the titanium lattice. In the present study, several grains along the crack are oriented with $(01\bar{1}0)$ parallel to the local crack path direction. When comparing the coordination number of bulk atoms in (0001) with $(01\bar{1}0)$, the surface free energy of (0001) is lower because it is more densely packed. Hence, adsorption of copper is more likely to occur on $(01\bar{1}0)$, since the driving force (potential reduction in energy) is higher. In addition, oxygen atoms are attracted to octahedral interstices in the hcp crystallographic structure, which are available in the crystallographic structure oriented $(01\bar{1}0)$. Thus by considering the atomic configuration in $(01\bar{1}0)$, adsorption of both copper and oxygen atoms is more likely to occur in that plane than in others such as (0001).

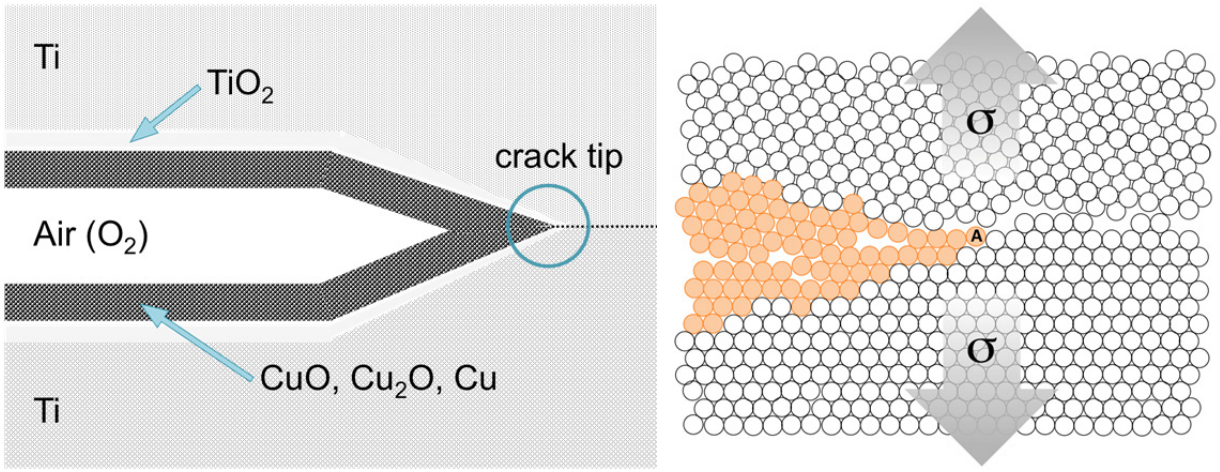

(a) **(b)**

Figure 5. (a) Schematic illustration of the crack wall and (b) the crack tip. Copper (and oxygen) enters the crack by surface self-diffusion and at the crack tip the copper atom "A" is adsorbed. The crack growth occurs under the tensile stress σ.

Another contributing reason to favourable crack growth along grains oriented close to [0001] in the crack direction (Y) could originate in the crystallography of titanium (alpha) and copper having hcp and fcc (face-centred cubic) structure, respectively. Studies of grain boundary segregation report that some grain boundaries are more prone to the segregation than others. Partly that is explained by the orientation relationship, that grain boundaries with preferable crystallography in relation to the segregate may be able to accommodate more segregates [29]. However, the work carried out in this area is limited, and no previous work has been done in this respect regard to SMIE of titanium. When studying hcp and fcc systems, four principal orientation relationships can be predicted [30], see figure 6, corresponding to the directions and planes in the hcp unit cell as given in figure 7.

With regard to SMIE, the orientation relationship could influence the crack path by attracting copper atoms to sites where they can adopt a structure similar to fcc. In figure 2 b), the crack path can be found along grains oriented in the directions $[10\bar{1}0]$ or $[11\bar{2}0]$ relative to the crack path, with one exception in the middle of the orientation map where the crack has propagated through a low angle boundary and across another grain, both oriented with (0001) parallel to the crack direction. However, the tendency of a favourable crack growth along grains orientated in the directions $[10\bar{1}0]$ and $[11\bar{2}0]$ relative to the crack path corresponds well with the hcp directions listed by the orientation relationships in figure 6. For instance, when $[10\bar{1}0]$ is parallel to [112] and (0002) is aligned with $(\bar{1}11)$ there is an orientation relationship between the hcp and the fcc crystallographic structure. Accordingly, for that specific crystallographic orientation, the atomic misfit between hcp and fcc is low, which enables the copper atoms to adopt a structure similar to fcc. Hence, as with segregation, a certain grain boundary orientation could attract and accommodate more copper, than another resulting in a heterogeneous distribution of copper atoms and thereby the crack growth might be preferable in certain directions.

$$\text{A:}\quad \left[1\bar{1}20\right]_{hcp}\left\|[110]_{fcc}\right. ,\quad (0002)_{hcp}/(\bar{1}11)_{fcc}$$

$$\text{B:}\quad \left[1\bar{1}20\right]_{hcp}\left\|[110]_{fcc}\right. ,\quad (1\bar{1}01)_{hcp}/(\bar{1}11)_{fcc}$$

$$\text{C:}\quad \left[10\bar{1}0\right]_{hcp}\left\|[112]_{fcc}\right. ,\quad (1\bar{2}10)_{hcp}/(\bar{2}20)_{fcc}$$

$$\text{D:}\quad \left[10\bar{1}0\right]_{hcp}\left\|[112]_{fcc}\right. ,\quad (0002)_{hcp}/(\bar{1}11)_{fcc}$$

Figure 6: Four predicted orientation relationships between the hcp (alpha titanium) and fcc (copper) systems.

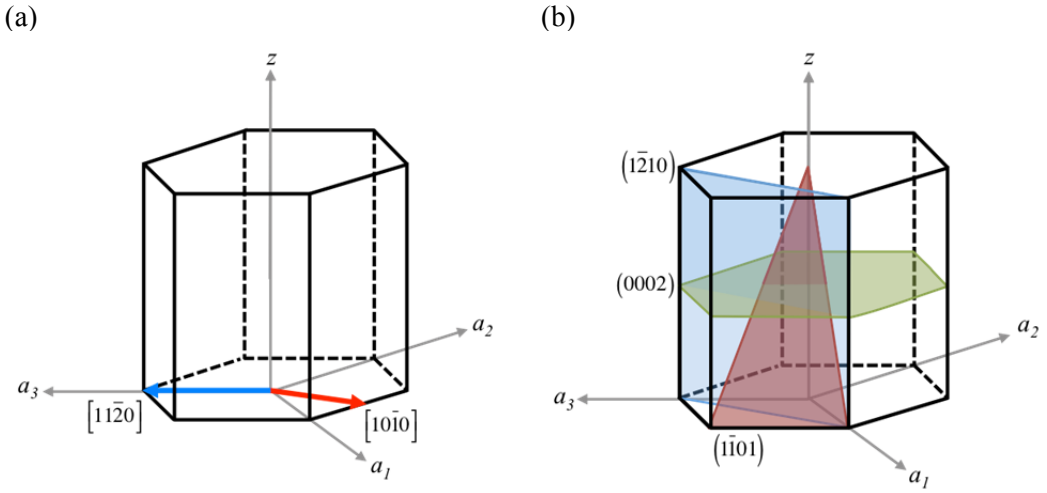

Figure 7. Orientation relationships in the hcp unit cell: (a) directions and (b) planes.

However, it is important to realise the complexity of adsorption; there are several theories that describe how the embrittling species weakens the crack tip region. The influence of adsorption on the crack tip will depend on the strength of adsorption, which in turn is dependent on several parameters, such as the surface energy and the solubility of the embrittling species in the matrix. Moreover, one should also keep in mind that the atomic bonds at the crack tip in the vicinity of atom "A" in figure 5 b), are strained by the tensile stress σ. Therefore, when the crack advances, crack growth is a result of both local stress and weakening of atomic bonds because of adsorption; depending on their magnitudes, the crack tip may experience either decohesion or dislocation emission.

5. Conclusions

The results of the present study agree with theories of surface self-diffusion and adsorption. Based on the observations of crack propagation path in relation to crystallographic orientation, the following conclusions can be drawn:

- Cracking in SMIE propagates principally along high-angle boundaries.
- Cracks propagate preferably along [0001] oriented grains in the crack direction, indicating that additional parameters influence the SMIE crack characteristics.

Acknowledgements
The authors would like to acknowledge Dr Dennis Lundström in the department of Materials Technology at GKN Aerospace Engine Systems for his practical assistance in the project, GKN Aerospace Engine Systems for the close collaboration and the graduate school in Space Technology for encouraging the project. Financial support from NFFP (the National Aviation Engineering Research Programme) is also highly appreciated.

References

[1] Kamdar M H 1983 Liquid Metal Embrittlement *Embrittlement of Engineering Alloys (Treatise on Material Science and Technology* vol 25) ed C L Briant and S K Banerji (London Academic Press) chapter 9 pp 362-455
[2] Lynch S P 1994 Failures of structures and components by environmentally assisted cracking *Eng. Failure Anal.* **1** 77-90
[3] Gordon P 1978 Metal induced embrittlement of metals – an evaluation of embrittler transport mechanism *Metallurgical Transactions A* **9** 267-73
[4] Lynch S P 1992 Metal-induced embrittlement of materials *Materials Characterization* **28** 279-89
[5] Kamdar M H 1985 Solid metal induced embrittlement of metals *Proc. of 6th International Conference on Fracture* (New Delhi) pp 3837-49
[6] Kamdar M H 1988 Solid metal induced embrittlement *J. Electrochem. Soc.* **37** 53-9
[7] Lynch S P 2008 Failures of structures and components by metal-induced embrittlement *Journal of Failure Analysis and Prevention* **8** 259-74
[8] Lynch S P 2003 Failures of engineering components due to environmentally assisted cracking *Practical Failure Analysis* **3** 33-42
[9] Kolman D G 2003 Solid metal induced embrittlement *ASM Handbook* ed S D Cramer and B S Convino (ASM International)
[10] Fager D N and Spurr W F 1970 Solid cadmium embrittlement: titanium alloys *Corrosion* **26** 409-19
[11] Lynch S P 1989 Solid-metal-induced embrittlement of aluminium alloys and other materials *Mater. Sci. Eng. A* **108** 203-12
[12] Lynn J C, Warke W R and Gordon P 1975 Solid metal-induced embrittlement of steel *Mater. Sci. Eng. A* **18** 51-62
[13] Westwood A R C and Kamdar M H 1963 Concerning liquid metal embrittlement, particularly of zinc monocrystals by mercury *The Philosophical Magazine* **8** 787-804
[14] Stoloff N S and Johnston T L 1963 Crack propagation in a liquid environment *Acta Metallurg.* **11** 251-6
[15] Westwood A R C, Preece C M and Kamdar M H 1967 Application of crack propagation criterion to liquid-metal embrittlement; cleavage of aluminium monocrystals in liquid gallium *Trans. Am. Soc. Metals* **60** 723-5
[16] Lynch S P 1981 Liquid-metal embrittlement in an Al 6%Zn 3%Mg alloy *Acta Materialia* **29** 324-40
[17] Lynch S P 1984 Metal-induced embrittlement of ductile materials and dislocation emission from crack tips *Scripta Metallurgica* **18** 509-13
[18] Lynch S P 1979 Mechanisms of fatigue and environmentally assisted fatigue *Fatigue Mechanisms* ed J T Fong (American society for testing and materials) pp 175
[19] Lynch S P 1978 Effect of environment on fracture – mechanisms of liquid-metal embrittlement, stress-corrosion cracking and corrosion-fatigue *Advances in Research on the Strength and Fracture of Materials* (Waterloo)

[20] Duttweiler R E, Wagner R R and Antony K C 1965 An investigation of stress-corrosion failures in titanium compressor components *Stress-Corrosion Cracking of Titanium: A Symposium Presented at the Fifth Pacific Area National Meeting* (Washington: ASTM) pp 152-78
[21] Stoltz R E and Stulen R H 1979 Solid metal embrittlement of Ti-6Al-6V-2Sn by cadmium, silver and gold *Corrosion* **35** 165-9
[22] Meyn D A 1973 Solid cadmium cracking of titanium alloys *Corrosion* **29** 192-6
[23] Liu D –X, Liu S –M and Fan G –F 2006 Investigation on behavior of solid copper-induced embrittlement of titanium alloy *J. Aeronaut. Mater.* **26** 1-5
[24] Åkerfeldt P, Pederson R and Antti M–L 2011 Solid metal induced embrittlement of titanium alloys in contact with copper *Proc. of The 12th World Conference on Titanium (Ti-2011)* (Beijing) pp 1868-71
[25] AMS 4916J 2006 Aerospace Material Specification: Titanium alloy sheet, strip, and plate 8Al-1Mo-1V duplex annealed (Warrendale: SAE International)
[26] Joshi V A 2006 Titanium Alloys – an Atlas of Structures and Fracture Features (Boca Raton, FL: Taylor and Francis Group)
[27] Åkerfeldt P, Pederson R and Antti M–L 2011 Investigation of the influence of copper welding electrodes on Ti-8Al-1Mo-1V and Ti-6Al-2Sn-4Zr-2Mo with respect to solid metal induced embrittlement *IOP conference series: Material Science and Engineering vol 31 (2012)*
[28] Shewmon P G 1998 Grain boundary cracking *Metallurgical and Materials Transactions: A* **29A** pp 1535-44
[29] Briant C L 2001 Grain boundary structure, chemistry, and failure *Materials Science and Technology* **17** 1317-23
[30] Zhang S, Chen H, Ren H and Kelly P M 2008 Crystallography of the simple HCP/FCC system *Metallurgical and Materials Transactions: A* **39A** 1077-86